Textile & Leather Review

ISSN 2623-6281 | www.tlr-journal.com | 10.31881/TLR

Fibre Blend and Web Arrangement for Optimized Dust-Holding, Hydrophobic, and Thermal Properties of Needle-Punched Nonwovens

Hanur Meku Yesuf, Syed Rashedul Islam, Direselgn Molla Semanie, Abdul Khalique Jhatial, Xueping Zhang, Xiaohong Qin

How to cite: Yesuf HM, Islam SR, Semanie DM, Jhatial AK, Zhang X, Qin X. Fibre Blend and Web Arrangement for Optimized Dust-Holding, Hydrophobic, and Thermal Properties of Needle-Punched Nonwovens. Textile & Leather Review. 2024; 7:988-1020. https://doi.org/10.31881/TLR.2024.047

How to link: https://doi.org/10.31881/TLR.2024.047

Published: 10 June 2024

Fibre Blend and Web Arrangement for Optimized Dust-Holding, Hydrophobic, and Thermal Properties of Needle-Punched Nonwovens

Hanur Meku YESUF[1,2], Syed Rashedul ISLAM[1,3], Direselgn Molla SEMANIE[1], Abdul Khalique JHATIAL[4], Xueping ZHANG[1*], Xiaohong QIN[1*]

[1]Key Laboratory of Textile Science & Technology, Ministry of Education, College of Textiles, Donghua University, Shanghai 201620, China

[2]Ethiopian Institute of Textile and Fashion Technology, Bair Dar University, Bahir Dar 6000, Ethiopia

[3]National Institute of Textile Engineering and Research (NITER), University of Dhaka, Dhaka 1350, Bangladesh

[4]Department of Textile Engineering, Mehran University of Engineering and Technology, Jamshoro, Sindh, Pakistan

*xhqin@dhu.edu.cn, xpzhang@dhu.edu.cn

Article

https://doi.org/10.31881/TLR.2024.047

Received 24 February 2024; Accepted 1 June 2024; Published 10 June 2024

ABSTRACT

$PM_{2.5}$ filters with hydrophobicity and thermal resistance are preferable for automobile cabins, engine air intake, and indoor applications, safeguarding against moisture ingress, microbial growth, and temperature fluctuations, and ensuring optimal air quality. This study explored the effects of blending five fibres with different web arrangements and fibre blend compositions on needle-punched dust-holding, hydrophobic, and thermal properties. Polyphenylene sulfide (PPS), polypropylene (PP), polyester (PET), polylactic acid (PLA), and polyacrylonitrile (PAN) were blended in different proportions to produce the samples. The method included opening, blending, carding, web laying, and needle punching to produce eight samples with cross-laid, parallel-laid, and pre-needled parallel-laid web configurations. Standard test methods were employed for the characterization. The results showed a dust holding capacity of > 3,423,000 particles/cm^2, the highest WCA of 133.12°, and the highest thermal resistance of 0.24255 m^{2}KW^{-1}. Based on the ANOVA analysis, web arrangement and pre-needling did not have a significant impact on the hydrophobicity of the samples. N0, N1, and N2 showed similar high water contact angles (~ 126°), indicating that the hydrophobicity was more affected by the chemistry of the fibre blend than by the web structure. Turkey's analysis of other samples strengthened this idea. However, they had a substantial impact on the porosity, air permeability, dust-holding capacity, and thermal properties at a P-value ≤ 0.05. The findings provide insightful information regarding the complex interactions among fibre content, web layout, and pre-needling to develop sophisticated needle-punched $PM_{2.5}$ filters.

KEYWORDS

blending, web-arrangement, needle-punched nonwoven, hydrophobic, thermal, dust-holding properties

INTRODUCTION

The utilization of multicomponent blends in the development of needle-punched nonwoven fabrics has emerged as a promising approach for achieving enhanced hydrophobic and thermal functionalities. Studies have shown that blending different fibres into nonwoven fabrics can lead to improved properties [1-6]. Additionally, the use of multi-fibre blends in needle-punched nonwoven fabrics demonstrated improved sound absorption properties, indicating their potential for acoustic product manufacturing [7,8]. Although needle-punched nonwovens offer effective $PM_{2.5}$ filtration, their hydrophobic properties are crucial for repelling water and certain liquid contaminants. Surface treatments such as fluoropolymers are used to enhance hydrophobicity [9-12]. However, these surface treatments degrade over time or under harsh conditions such as UV exposure or chemical attack. This compromises the filter's repellency and overall performance. Certain fluoropolymer-based treatments also raise concerns regarding potential environmental and health risks. Their production and disposal contribute to greenhouse gas emissions and PFAS contamination. Studies have outlined the environmental and health concerns associated with fluoropolymers, urging for safer alternatives [13-17].

The selection of fibres based on their specific hydrophobic and thermal properties can address specific needs. The hydrophobic properties of polyacrylonitrile (PAN) play a major role in $PM_{2.5}$. PAN-based nanofibre filters exhibit a low-pressure drop and excellent filtration efficiency. Examples of these filters include PAN/PVP blend nanofibre filter media [18] and electreted polysulfonamide/polyacrylonitrile-boehmite (PSA/PAN-B) composite nanofibre filters [19]. The hydrophobicity of PAN allows for the effective capture of particulate matter through dipole-dipole intermolecular forces [20]. Additionally, the hydrophobicity of PAN-based filters enables them to maintain high filtration efficiency, even under high-humidity conditions [21]. Overall, the hydrophobic properties of PAN play a crucial role in enhancing the capture efficiency and performance of $PM_{2.5}$ filters in harsh environments.

PAN is a high-performance fibre with good heat-resistance properties. In a review [22], it was mentioned that recycled oxidized PAN exhibited high residue formation with stability up to 1500 °C. This indicates that PAN can withstand high temperatures without significant degradation, making it suitable for applications in which heat resistance is important. In another study, the authors mentioned that PAN fibres can influence the thermal stability of composites, as demonstrated by Thermogravimetric Analysis (TGA) results, where PAN-based composites exhibited better thermal stability [23]. On the other hand, studies [24] have shown that polyacrylonitrile (PAN) is a versatile polymer that is commonly used in the production of electrospun webs to create superhydrophobic self-cleaning surfaces. PAN fibres have been extensively studied [25] for their robustness, chemical resilience, and thermal endurance, particularly in the development of protective membranes known for their multifunctional attributes, including superhydrophobicity, self-cleaning capabilities, UV resistance, and integration into self-powered systems. PAN is a less hydrophobic polymer with good chemical resistance and is suitable for separation membranes in contrast to the hydrophobic nature of polypropylene (PP) and polyphenylene sulfide (PPS) [26].

Huijing et al. developed a water-repellent and lipophilic composite needle-punched nonwoven fabric by blending PET and polyolefin fibres, resulting in improved water-repellency and tensile strength [2]. The combination of viscose and polyester fibres in nonwoven industrial wipes fabricated using the needle-punching technique was studied, and it was found that a higher polyester fibre content led to a reduction in the vertical wicking rate [27]. Huijing and Zhang discussed in their article the utilization of multi-fibre blends, specifically blending PET fibre with polyolefin fibre, to enhance the water-repellency of needle-punched nonwoven fabrics [28].

Tahir et al. evaluated the potential of bamboo/polyester-blended needle-punched nonwoven batts as thermal insulators to investigate the effects of physical properties on thermal resistance and bursting strength [29]. Incorporating hydrophobic and thermally resistant polyesters in the construction of needle-punched $PM_{2.5}$ filters enhances their efficiency by providing both water resistance and resilience to temperature variations. This dual functionality ensures the durability of the filter, making it effective under diverse environmental conditions, while maintaining its filtration performance. Filter bags are made of standard-grade polyester needle felt with a calendared surface finish to filter dust emissions in the $PM_{2.5}$ range [30]. A polyester filter medium was used for surface treatment to improve its ability to attract and hold dust particles [31].

A study [32] on the performance of needle-punched nonwoven fabrics incorporating polylactide (PLA) fibres, which are renowned for their biodegradability and sourced from renewable materials such as corn starch or sugarcane, alongside *Triumfetta cordifolia* (TC) fibres, resulted in the favourable mechanical performance of the nonwoven fabrics. Studies [33,34] have highlighted the emerging applications of PLA polymers, particularly in enhancing filtration efficiency through triboelectric media and in various filter applications, including the automotive and chemical industries, as well as single-use applications, owing to the unique properties of PLA fibres, such as their electropositivity and suitability for disposable filters. A study [35] demonstrated that jute/PLA composites exhibit promising tensile, flexural, and thermal properties, suggesting their potential for application in diverse industries, including automotive, aviation, construction, and home decor, owing to their favourable attributes of low density, cost-effectiveness, and biodegradability. PLA can be either slightly hydrophilic (water-attracting) or hydrophobic. Generally, pure PLA is considered less hydrophobic with a lower WCA [36].

The effects of fabric weight, needling density, and blend proportion of nettle and polypropylene fibres on oil sorption have also been investigated, indicating their potential for enhancing the hydrophobic properties [37]. Another study reported that the thermal insulation properties of nonwoven fabrics made from kapok/polypropylene blends with 70/30 blend ratios exhibited the highest thermal resistance [38].

Composite membranes made of polypropylene, polyvinyl alcohol, and metal-organic framework have a high level of filtration effectiveness and are intended to efficiently filter out $PM_{2.5}$ [39]. In a recent study, researchers investigated the impact of polypropylene nonwoven microfibre substrate thickness on the air filtration performance of a polyacrylonitrile nanofibre material to clarify the connection between the substrate thickness and the effectiveness of air filtration by the nanofibre membrane [40].

Zhao et al. fabricated a filter from aramid fibres enhanced by ultrafine PPS fibres. This enhancement improves the filter performance in terms of thermal stability and chemical resistance [41]. The use of PTFE and PPS materials in filters ensures high thermal and chemical resistance, making them suitable for various applications where exposure to extreme temperatures or harsh chemicals is a concern [42]. A study [43] demonstrated that modifying polyphenylene sulfide (PPS) nonwoven fabric with a polybenzoxazine precursor coating enhances its thermal and oxidation resistance, resulting in improved tensile strength and Young's modulus, increased hydrophobicity, superior environmental stability, and enhanced filtration performance.

Hydrophobic and thermal resistance are crucial properties for $PM_{2.5}$ filters used in various applications, including automobile cabin and engine filters as well as indoor filters [44, 45]. Automobile cabin filters [46-49], are used to repel moisture, prevent microbial growth, and withstand diverse temperature fluctuations experienced within vehicles. Similarly, engine air intake filters [50-52], played the same role against moisture and oil vapour ingress and withstood the high temperatures encountered near the engine. These properties also prevent clogging and ensure reliable filtration without degradation, safeguard against engine damage, or reduce efficiency. In indoor filters [53-56], hydrophobicity prevents the growth of mould and mildew by repelling moisture, thereby maintaining clean and breathable indoor air quality. Furthermore, the thermal resistance in indoor filters enables them to withstand temperature variations, particularly in industrial or commercial settings, ensuring consistent performance under diverse conditions. Overall, above mentioned $PM_{2.5}$ filters are durable, and efficient, and provide air quality in automotive cabins, engine air intake systems, and indoor spaces. In this study, polyester (PET), polypropylene (PP), polyacrylonitrile (PAN), polylactic acid (PLA), and polyphenylene sulfide (PPS) were not selected randomly; rather, they were deliberately chosen from the numerous fibres utilized in the manufacturing of needle-punched nonwoven fabrics. FTIR analysis of the sample nonwovens, referenced in our previous publication

[1], confirmed the presence of all fibres within the sample structure. Hydrophobic and moisture-wicking fibres like PP, PET, and PPS are blended to control the amount of moisture in the nonwoven filter and minimise liquid buildup that can impair filtration efficiency. In the same instance, enhancing the thermal insulation of nonwoven materials is accomplished by blending fibres with various thermal characteristics, such as PPS, PAN, PET, and PLA. Low-heat-conductivity fibres such as PLA and PET are also blended to aid in lower heat transfer through the needle-punched filter and to preserve a steadier temperature inside the filtration system.

EXPERIMENTAL

Materials

The development of needle-punched nonwoven materials involved the incorporation of five distinct fibres, polyphenylene sulfide (PPS), polylactic acid (PLA), polyester (PET), polypropylene (PP), and polyacrylonitrile (PAN) staple fibres, each with an equal blending percentage. Suzhou Makeit Technology Co. (Suzhou, China) was used as the fibre supplier. Table 1 provides an inventory of fibre specifics [1].

Table 1. Basic properties of fibres

Parameters	Unit	Fibre type				
		PAN	PET	PLA	PP	PPS
Fibre Length	mm	38	38	51	51	51
Fibre Fineness	dtex	1.3	1.56	6.66	2.22	1.53
Fibre Strength	cN/dtex	5.62	5.42	0.44	2.83	6.31
Elongation	%	14.26	13.88	2.24	18.65	24.78
Density of fibre	g/cm^3	1.17	1.38	1.26	0.91	1.36

Sample Preparation

In this study, polyphenylene sulfide (PPS), polylactic acid (PLA), polyester (PET), polypropylene (PP), and polyacrylonitrile (PAN) fibres were opened and blended in different proportions (Table 2). A schematic of the blending, web-laying, pre-needling, and final needling processes is shown in Figure 1. The blended fibres were processed using a carding machine with a constant feed roller, cylinder, and doffer speed. For every web, the feed weight remained constant at 100 g. For every sample, six webs were made with equal fibre blend percentages by weight; these webs were then laid down in three distinct ways immediately after carding to create three distinct pieces of needle-punched nonwoven material. Sample N0 had alternating machine and cross-directional fibre web alignment, whereas samples N1 – N7 predominantly had machine-directional web alignment for increased homogeneity. Carding parameters, including feeder speed, cylinder speed, and doffer speed, were consistent for sample preparation.

Table 2. Fibre blend compositions and web arrangement

Samples	N0, N1, N2	N3	N4	N5	N6	N7
Fibre blend composition	[1]	60% PAN 10% PET 10% PLA 10% PP 10% PPS	10% PAN 60% PET 10% PLA 10% PP 10% PPS	10% PAN 10% PET 60% PLA 10% PP 10% PPS	10% PAN 10% PET 10% PLA 60% PP 10% PPS	10% PAN 10% PET 10% PLA 10% PP 60% PPS
Web arrangement	[1]	Six webs laid down in a parallel-laid manner one on top of the other				

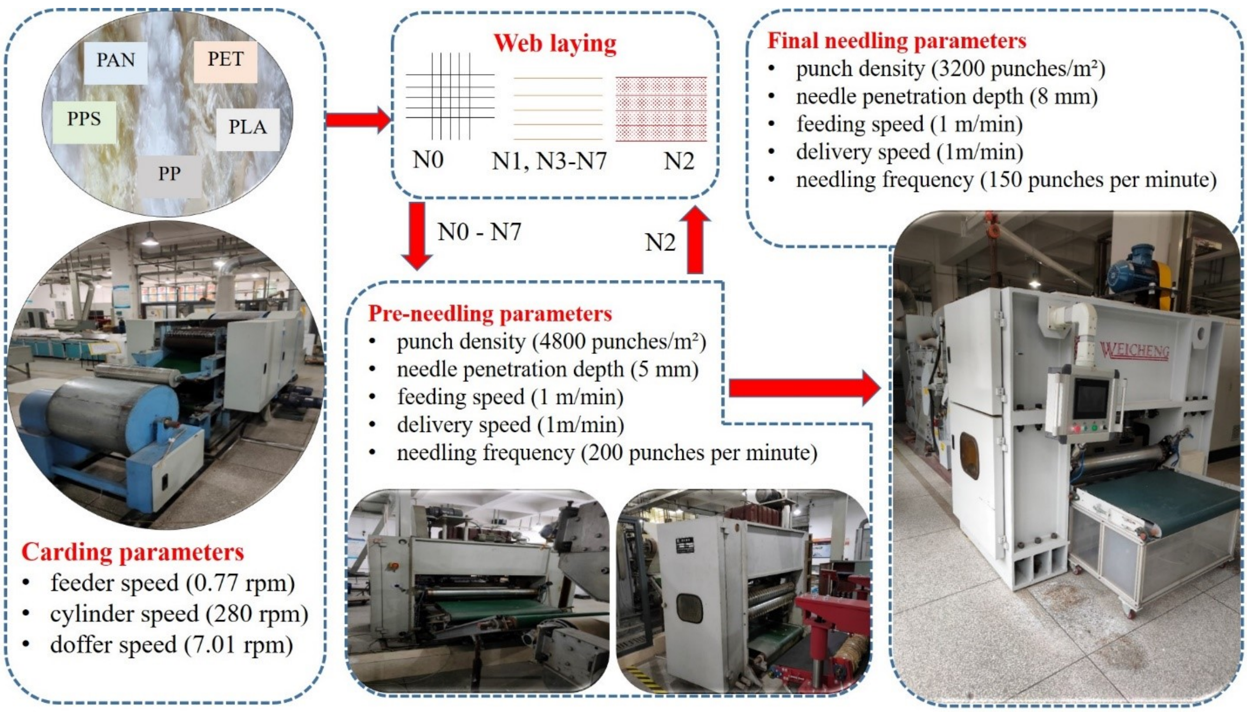

Figure 1. Blending, web laying, pre-needling and final needling processes

The final webs underwent pre-needling and final needling punch processes to entangle the fibres. Pre-needling was employed to create a preliminary 3D web and minimize the web thickness. The samples were then passed through the main needle-punching loom, with sample N2 undergoing additional pre-needling steps before web-laying for enhanced compression. For both pre-needling and final needling, parameters such as punch density, needle penetration depth, feeding speed, delivery speed, and needling frequency were specified. Sample N2 underwent eight needling processes, whereas the other samples underwent six needling processes. This information has been explained clearly in our previously published paper [1].

Characterization

Standard test methods

The test and experimental procedures were performed according to the standard test method. Before the test, all the samples were conditioned under a standard atmosphere at a temperature of 20 ± 2 °C and a relative humidity of 65% for 24 h.

SEM Analysis

A Flex-SEM 1000 (SU1000, Hitachi Ltd. Japan) was used for scanning electron microscopy (SEM) to analyze the morphology of the fibres and samples. For every fibre and needle-punched sample, a vacuum sputter coater was used to apply a gold coating before examination.

Porosity

The porosity h of the needle-punched nonwoven fabric, defined as the ratio of open space to the total volume of the porous material, was calculated from the measured fabric thickness and weight per unit area. The porosity values of three samples of needle-punched nonwoven fabrics were calculated according to ASTM C 830-00 Standard Test Methods for Apparent Porosity, Liquid Absorption, Apparent Specific Gravity, and Bulk Density of Refractory Shapes by Vacuum Pressure using Equation (1) [57-59].

$$\mathrm{h} = \left(1 - \frac{\rho_{\mathrm{w}}}{\rho_{\mathrm{f}}}\right) * 100 \tag{1}$$

Where h is porosity, ρ_w is the density of the fabric, and ρ_f is the density of the fibre.

Air Permeability

The air permeability test, as per the relevant provisions of ASTM D737–96, determines the velocity of airflow passing perpendicularly through a test specimen under specific conditions. These standardized conditions ensured consistent and comparable measurements of air permeability for the various fabric samples. Air permeability is defined as the rate of airflow through a designated area of the fabric measured at a given pressure difference and over a specified time. The test was performed using a YG461E automatic air permeability tester, with the test surface area set at 20 cm^2. A pressure drop of 200 Pa was applied across the fabric test area during testing.

Dust Holding Capacity

An automatic digital tester called the U-Test (Model: F003, Uti Intelligent Technology Co., Ltd., Suzhou, China) was used to measure the dust holding capacity. To induce dust, NaCl particles of $PM_{2.5}$ were added to the filtering system at a steady air pressure flow rate of 32 l/min, following the ISO 29463 evaluation system. At 20 °C temperature and 45% relative humidity, the tests were assessed. Following this, Equation (2) was used to determine the dust holding capacity [60].

$$D_h = \frac{D_c \text{ x } D_f}{F_A} \text{ x } 100 \quad (2)$$

Where D_h is dust holding capacity (particles/cm^2), D_c is dust collected, D_f is dust fed, and F_A is filter area (cm^2).

Water Contact Angle

An optical video contact angle device (Model KINO SL200KS) was used to measure the water contact angle. A 10-millilitre droplet of water was applied to the samples, and the water contact angle was measured for 180 s. Every sample showed an average of five distinct zones for every contact angle. The test temperature was maintained at 20 °C.

Thermal Resistance

The thermal insulation characteristics of the needle-punched fabrics were assessed using a YG606E thermal resistance tester (China). According to GB/T 11048-2008 standard, the testing plate was maintained at a temperature of 35 °C. Each sample underwent three measurements, and the average values were calculated. Thermal resistance, a measure of a material's ability to impede heat flow, was substantiated by assessing the heat properties and extent of temperature variation within the material. The higher fabric density and presence of entrapped air within the fabric structure contributed to the increase in thermal resistance. The surface of the needle-punched fabric consisted of pores enclosed by fibres. Thermal resistance is influenced by factors such as thermal conductivity and thickness of the needle-punched nonwoven fabric. The relationship between thermal resistance and thermal conductivity is defined by Equation (3) [61,62].

$$R = \frac{T}{\lambda} \tag{3}$$

Where R is thermal resistance in m^2KW^{-1}, T is the fabric thickness in m, and λ is thermal conductivity in $Wm^{-1}K^{-1}$.

Differential scanning calorimetry (DSC)

DSC experiments were conducted to analyze the thermal properties of a needle-punched nonwoven $PM_{2.5}$ filter composed of Polyacrylonitrile (PAN), Polylactic acid (PLA), Polyester (PET), Polypropylene (PP), and Polyphenylene Sulfide (PPS). The experiments utilized the PerkinElmer DSC 4000 machine. The nonwoven samples were subjected to a controlled heating rate of 20 °C per minute, with the temperature range extending from 5 °C to 400 °C.

Shrinkage or Dimensional Stability

Three random samples were obtained for each MD and CD (ISO 3005:2015). The samples measured 60 mm wide and 120 mm long. In the MD and CD, two lines were drawn perpendicular to each other. The lengths of each line were 60 mm and 40 mm in the longer and shorter directions, respectively. Each sample was kept in an oven for a full day at 150 °C. The following method was used to compute the after-shrinkage, which was determined after the samples were conditioned for 24 h. The recorded values were used to calculate the shrinkage percentage of the needle-punched nonwoven filter samples using Equation (4) [60].

$$S = \frac{L_b - L_a}{L_b} \text{ x } 100 \tag{4}$$

Where S is shrinkage percentage (%), L_b is length before (mm), and L_a is length after (mm).

RESULTS AND DISCUSSION

Scanning Electron Microscopy

As shown in Figure 2, scanning electron microscopy (SEM) revealed the surface morphological structures of the fibres and needle-punched nonwoven samples. The variations in fibre length and fineness between fibres such as those measuring 38 mm and 51 mm in length and with fineness ranging from 1.3 to 6.66 dtex were shown in Figure 2 (a-e) and Table 1, significantly impact the properties of needle-punched samples, particularly in terms of hydrophobicity, $PM_{2.5}$ filtration efficiency, and thermal characteristics. Longer fibres tend to offer better interlocking and entanglement within the nonwoven structure, potentially enhancing mechanical strength and durability. Short fibres, acting as fillers, contribute to a denser and more uniform fabric structure by filling the gaps between longer fibres, as shown in Figure 2 (f-h), indicated by white ellipses. This structural improvement resulted in reduced air permeability and increased dust-holding capacity, demonstrating the crucial elements for effective $PM_{2.5}$ filtration.

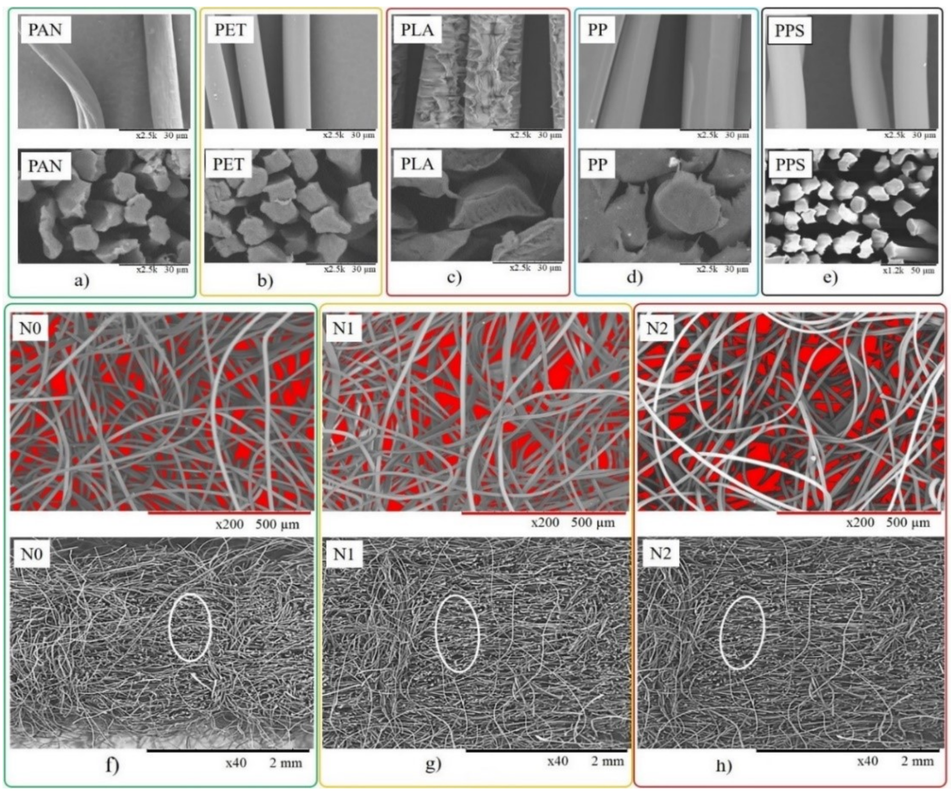

Figure 2. SEM images of fibres and needle-punched samples; fibre surface (top figures) and cross-sectional (bottom figures) views: a) PAN, b) PET, c) PLA, d) PP, e) PPS; needle-punched nonwoven sample surface (top figures) and cross-sectional (bottom figures) views: f) N0, g) N1, and h) N2

Short fibres also play a role in preventing larger particles from prematurely clogging the filter. Finer fibres with smaller diameters contribute to an increased surface area and improved packing density, thereby affecting properties such as hydrophobicity and filtration efficiency. Additionally, variations in fibre length and fineness also influence the pore structure and surface morphology of the nonwoven material, as in the top layers shown in Figure 2 (f-h), indicated by red shades, ultimately affecting its air permeability. In general, the deliberate blending of fibres with diverse lengths and fineness has emerged as a valuable strategy for engineering needle-punched $PM_{2.5}$ filter nonwovens with superior hydrophobic and thermal properties, and optimal filtration performance by repelling water, capturing fine particles, and providing thermal resistance.

Porosity, Air Permeability and Dust Holding Capacity

The porosity, air permeability, and dust-holding capacity of needle-punched nonwoven samples are shown in Figure 3. N0 (cross-laid web arranged) exhibited the lowest porosity (89.96%), consistent with its low air permeability. The cross-web arrangement and high fabric density contributed to the fabric having fewer voids. N1 (parallel-laid arrangement) showed a higher porosity (92.47%) than N0, in line with its higher air permeability. The parallel arrangement and medium fabric density contributed to the more porous structure. N2 (pre-needled and parallel-laid arranged) displayed slightly higher porosity (93.11%) compared to N1, suggesting that pre-needling and parallel arrangement, even with relatively less fabric density, resulted in a fabric structure with slightly increased porosity.

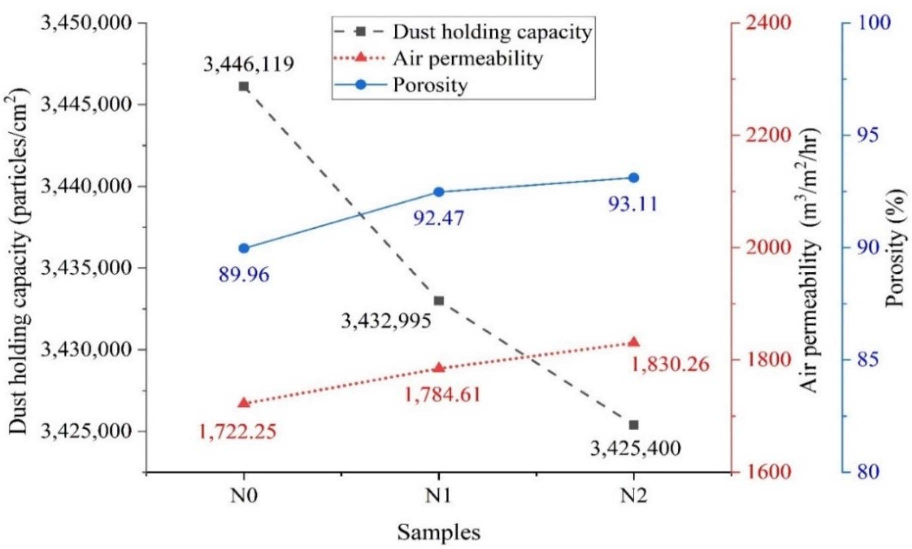

Figure 3. Air permeability, porosity and dust holding capacity of needle-punched nonwoven samples

N0 exhibited the lowest air permeability (1,722.25 $m^3/m^2/hr$), suggesting that the cross-web arrangement and high fabric density created a less porous structure, limiting the ease with which air could pass through. N1 showed significantly higher air permeability (1,784.61 $m^3/m^2/hr$) compared to N0. The parallel arrangement and medium fabric density contributed to a more open structure, allowing air to pass more readily. N2 displayed the highest air permeability (1,830.26 $m^3/m^2/hr$) among the three samples,

https://doi.org/10.31881/TLR.2024.047

indicating that the pre-needling and parallel arrangement resulted in a fabric structure with high permeability.

The substantial dust holding capacity (3,446,119 particles/cm^2) of N0 suggested that the combination of the cross-web arrangement and higher fabric density allowed for effective dust retention. N1's substantial dust holding capacity (3,432,995 particles/cm^2) recommended efficient particle capture supported by a balanced fibre composition and fabric structure. N2's substantial dust-holding capacity (3,425,400 particles/cm^2) suggested effective dust retention.

Likewise, the commercial needle-punched PPS [60] (GSM 560 g/m2) displayed a filtration effectiveness of 95.8%, along with a dust holding capability of 212 g/m^2, a pressure drop of 7.5 bar, an air permeability of 105 l/m^2/s, and thermal shrinkage of below 1%. Moreover, a commercial needle-punched PPS/PI [60] (560 g/m^2) showed a filtration efficiency of 95.6%, dust holding capacity of 211 g/m^2, pressure drop of 3.13 bar, air permeability of 155 l/m^2/s, and thermal shrinkage of less than 1%. The findings of our study closely mirror these industry benchmarks. This study examined the porosity, air permeability, and filtration characteristics of needle-punched nonwoven samples (N0, N1, and N2) with varying fibre arrangements and blend compositions. The arrangement of fibres and pre-needling processes affected the air permeability and porosity, with parallel arrangements resulting in higher values. On the other hand, higher fabric density enhanced filtration efficiency and dust-holding capacity. The balanced combination of fabric density, thickness, web arrangement, and fibre properties plays a crucial role in determining the dust-holding capacity, emphasizing the need for a tailored approach to filtration requirements.

Water Contact Angle

The hydrophobic properties of needle-punched nonwoven samples are shown in Figure 4. The water contact angles of the samples are presented in Figure 4 (a-c), and the actual water droplets on the surfaces of the samples are shown in Figure 4 (d-f). N0 exhibited a relatively higher water contact angle of 126.77°, suggesting hydrophobic characteristics. The cross-web arrangement, higher fabric density, and lower thickness contribute to the hydrophobic nature of the fabric. The higher fabric density and lower thickness in N0 potentially enhanced the hydrophobicity, providing a compact and less porous structure that resists water penetration. N1 showed a slightly lower water contact angle of 126.47° compared to N0. The parallel arrangement and moderate fabric density and thickness contributed to the balanced hydrophobicity. N2 demonstrated a moderate water contact angle of 126.56°, influenced by the pre-needling process, parallel arrangement, and fabric characteristics. The lower fabric density and higher thickness in N2 combined with pre-needling contributed to moderate hydrophobicity, indicating potential water-repellent properties.

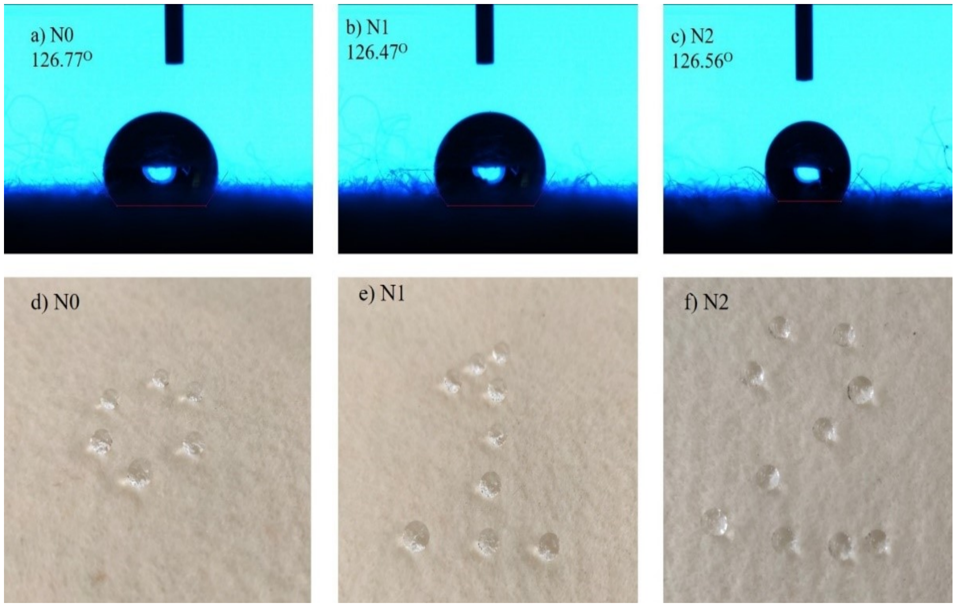

Figure 4. Hydrophobic properties of needle-punched nonwoven samples: water contact angle of needle-punched nonwoven samples (a-c), water droplets on the surfaces of needle-punched nonwoven samples (d-f)

The cross-web arrangement in N0 contributed to a higher water contact angle, indicating better water repellency. The parallel arrangement in N1 and N2 showed a slightly lower water contact angle, suggesting different interactions with water. Water contact angle measurements indicated the hydrophobic nature of needle-punched nonwoven fabrics. The combination of fabric density, thickness, web arrangement, and fibre properties influences the water-repellency of fabrics. N0, with a cross-web arrangement and higher fabric density, exhibited the highest water contact angle, suggesting superior water repellency. N1 and N2 exhibited slightly lower water contact angles, reflecting their respective arrangements and fabric characteristics. The hydrophobicity observed in all samples could be advantageous in applications where water resistance is desired.

PAN fibres exhibited hydrophobic properties, contributing to their water repellency. The molecular structure of PAN, which contains carbon and nitrogen atoms, results in a hydrophobic surface. The polyester and PP polymer structure inherently resisted water absorption, making the polyester and PP-based fabric water-repellent. In particular, the non-polar nature of polypropylene contributed to its water-repellent characteristics and was resistant to wetting. PPS exhibits excellent resistance to chemicals, high temperatures, and moisture. The inclusion of PPS in the fibre blend contributed to the overall hydrophobicity of the fabric, potentially influencing properties such as water repellency and resistance to moisture absorption. Blending these fibres in equal proportions allowed for a combination of their hydrophobic characteristics. The resulting needle-punched nonwoven fabric benefited from the collective hydrophobicity of PAN, PET, PP, and PPS, providing resistance to water absorption and enhancing water repellency.

Thermal Properties

Thermal Resistance

Comprehensive insights into the thermal behaviour of the materials with fabric density, porosity and air permeability of samples N0, N1, and N2, are presented in Table 3. Sample N0, with a cross-web arrangement and the highest fabric density (121.34 Kgm^{-3}) exhibited the highest thermal resistance (0.21053 m^2KW^{-1}). The dense arrangement contributed to effective thermal insulation, which is a crucial factor for retaining heat and maintaining filtration efficiency.

Sample N1, with a parallel arrangement and a lower fabric density of 90.96 Kgm^{-3} showed an intermediate thermal resistance (0.20820 m^2KW^{-1}). The parallel arrangement and lower fabric density maintained a balance between the thermal performance and filtration efficiency. Sample N2, pre-needled and parallel arranged with the lowest fabric density of 83.40 Kgm^{-3} exhibited the lowest thermal resistance (0.19914 m^2KW^{-1}) among the three samples. The pre-needling process and lower fabric density contributed to a lower thermal resistance, which may have implications for heat dissipation in filter applications. N2 also possessed the highest porosity of 93.11%. As the porosity increased, the density of the material decreased because the void spaces displaced the solid materials. At a lower density, there was less resistance to the flow of heat, which meant that the material became more conducive to heat flow.

Table 3. Thermal resistance properties of needle-punched nonwoven samples

Sample	Fabric density ($Kg\ m^{-3}$)	Air permeability ($m^3/m^2/hr$)	Porosity (%)	Thermal resistance (m^2KW^{-1})
N0	121.34	1,722.25	89.96	0.21053
N1	90.96	1,784.61	92.47	0.20820
N2	83.40	1,830.26	93.11	0.19914

Polyphenylene sulfide (PPS), polypropylene (PP), polyester (PET), polylactic acid (PLA), and polyacrylonitrile (PAN) fibres play a crucial role in influencing the fabric properties, including thermal conductivity and resistance. Equal proportions of these fibres were blended to obtain a uniform distribution of thermal resistance across the material. The interactions between the fibres affected the pathways for heat flow and the overall resistance to thermal transfer. Polyester (PET), known for its versatility and strength, shows thermal resistance that aligns with its application in textiles and other materials. Polylactic acid (PLA), which is derived from renewable resources, often exhibits thermal resistance that is appropriate for use in biodegradable and environmentally friendly materials. Polyacrylonitrile (PAN) is a synthetic polymer that typically exhibits moderate thermal resistance. Polyphenylene sulfide (PPS), which is known for its high-temperature stability, displays excellent thermal resistance, permitting it to withstand harsh environments.

Differential Scanning Calorimetry (DSC) Analysis

Differential scanning calorimetry (DSC) experiments were conducted on a needle-punched nonwoven $PM_{2.5}$, filter composed of PAN, PLA, PET, PP, and PPS, at a heating rate of 20°C/min and a temperature range from 5 to 400 °C. The DSC graph shown in Figure 5 reveals distinct peaks corresponding to the thermal behaviour of each component. Insights gained from the DSC analysis included the confirmation of the presence of all five fibres (PLA, PP, PET, PAN, and PPS) in the three samples N0, N1, and N2 needle-punched nonwoven materials, aligned with the expected blend composition. The DSC analysis of the needle-punched nonwoven $PM_{2.5}$ filter samples (N0, N1, and N2) with distinct web arrangements (cross-laid, parallel-laid, and pre-needled parallel-laid) revealed remarkably similar thermal characteristics. The observed peaks, including the melting temperatures of the individual fibres (PAN, PLA, PET, PP, and PPS), were consistent across all three samples. This uniformity in thermal behaviour suggests that the different web arrangements had a minimal impact on the thermal transitions of the fibres within the needle-punched nonwovens.

The consistency in peak shapes and temperatures indicated that the web arrangement, whether cross-laid, parallel-laid, or pre-needled parallel-laid, did not significantly alter the molecular interactions or blending of fibres at the thermal level. Equal proportions of PAN, PLA, PET, PP, and PPS fibres in each sample combined with the needle-punching process appeared to homogenize the thermal characteristics, leading to similar DSC profiles. While the web arrangement played a crucial role in the mechanical and physical properties of needle-punched nonwoven fabrics, the DSC results suggested that it might not exert a pronounced influence on the thermal transitions of individual fibres in this specific needle-punched nonwoven fabric. This finding emphasizes the robustness of the needle-punching process in creating a uniform distribution of fibres and thermal properties, irrespective of the initial web arrangement.

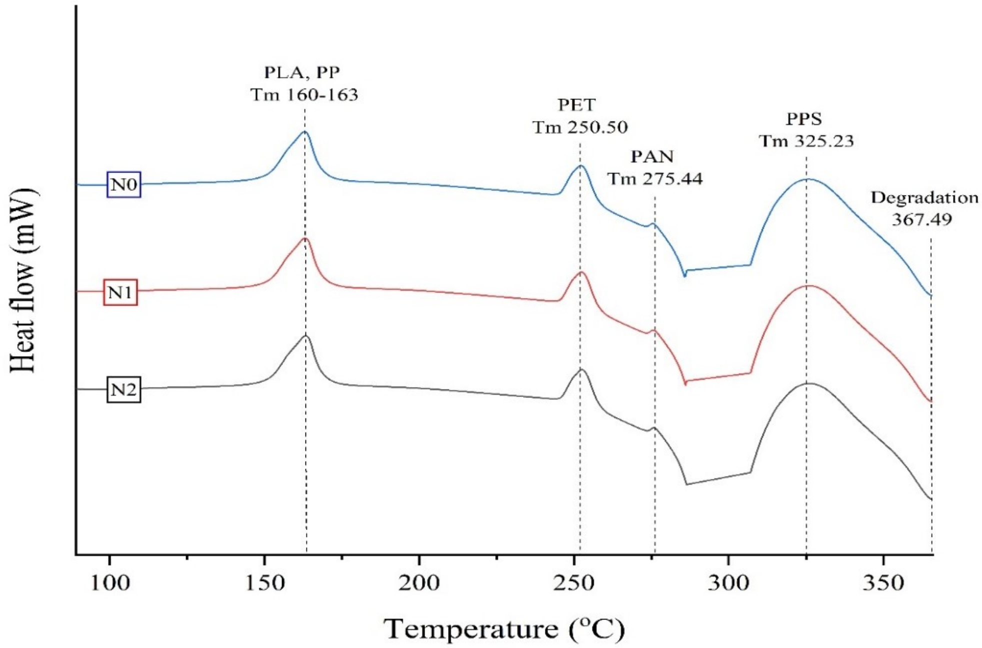

Figure 5. DSC results of needle-punched nonwoven samples

The distinct melting peaks reveal a clear separation of the thermal transitions for each fibre. Notably, PLA and PP displayed endothermic peaks with a melting temperature (Tm) range of–160-163 °C. PET showed an endothermic peak at Tm 250.50 °C, while PAN showed a higher Tm at 275.44 °C. PPS exhibited the highest Tm among all the components, with an endothermic peak at 325.23 °C. Moreover, an incident degradation was observed at 367.49 °C. These endothermic peaks signify heat absorption during processes, such as melting or glass transition. DSC analysis of the needle-punched nonwoven $PM_{2.5}$ filter revealed numerous different endothermic peaks. The broad peak in the range of 160-170 °C is attributed to the melting of PLA and PP fibres, given their overlapping melting temperature ranges. The smaller peak at approximately 250 °C aligns with the melting temperature range of PET. The shoulder peak at 275 °C is indicative of the melting of PAN, while the broad peak at approximately 325 °C corresponds to the highest melting fibre, PPS, in the blend.

The absence of significant exothermic peaks in the DSC curve indicates good thermal stability of the material. However, a notable exothermic peak was observed at 367.49 °C, signifying the onset of thermal degradation of the blended nonwoven material. The lower intensity of the PAN peak, compared to those of PLA/PP and PET, was attributed to its higher melting temperature, resulting in slower heat absorption at the chosen heating rate of 20 °C/min. The observed thermal stability was encouraging, with no exothermic peaks observed until a relatively high degradation temperature.

Shrinkage or Dimensional Stability

The fabric shrinkage in the cross direction (CD) was reported to be 0% for N0, N1, and N2, as shown in Figure 6. The needle-punched nonwoven samples for the $PM_{2.5}$ filter exhibited consistent dimensional stability across all three arrangements (N0, N1, and N2), as indicated by the zero per cent shrinkage in both directions. This uniformity in shrinkage suggests that the web arrangements, whether cross-laid, parallel-laid, or pre-needled parallel-laid, did not significantly affect the dimensional stability of the samples.

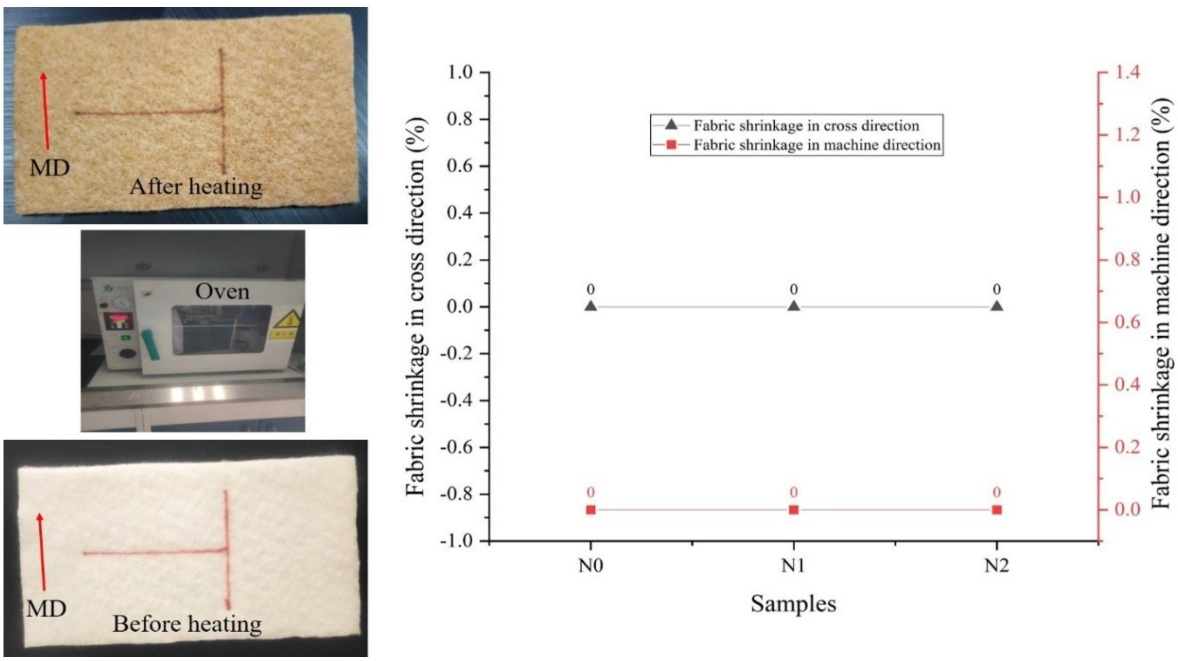

Figure 6. Shrinkage of needle-punched nonwoven samples

The uniform dimensional stability of the samples was maintained by blending equal proportions of polyphenylene sulfide (PPS), polypropylene (PP), polyester (PET), polylactic acid (PLA), and polyacrylonitrile (PAN) fibres. PAN and PET had higher shrinkage tendencies than PLA and PP, while PPS is known for its excellent heat resistance and minimal shrinkage. However, owing to the equal blend, the shrinkage can be optimized throughout the sample fabrics. In general, the lack of shrinking highlights the appropriateness of the needle-punched nonwoven samples for $PM_{2.5}$ filter applications by guaranteeing that they will retain their original size and form while in use.

Relationship between Fabric Density, Air Permeability and Porosity

The linear fit relationship between density, air permeability, and density with the porosity of needle-punched nonwoven samples is presented in Figure 7 (a) and Table 4. The linear fit analysis between the fabric density (x) and air permeability (y) yielded Equation (5). This equation proposes that as the fabric density increases, the air permeability decreases, with a coefficient of -2.6. The coefficient of determination (R^2) for this linear fit was 0.885, indicating that approximately 88.5% of the variability in air permeability can be explained by the change in fabric density. The linear fit analysis between the fabric density (x) and porosity (y) yielded Equation (6). This equation indicates that as the fabric density increases, the porosity decreases, with a coefficient of -0.08. The coefficient of determination (R^2) for this linear fit was 1, indicating a perfect fit, in which 100% of the variability in porosity was explained by altering the fabric density.

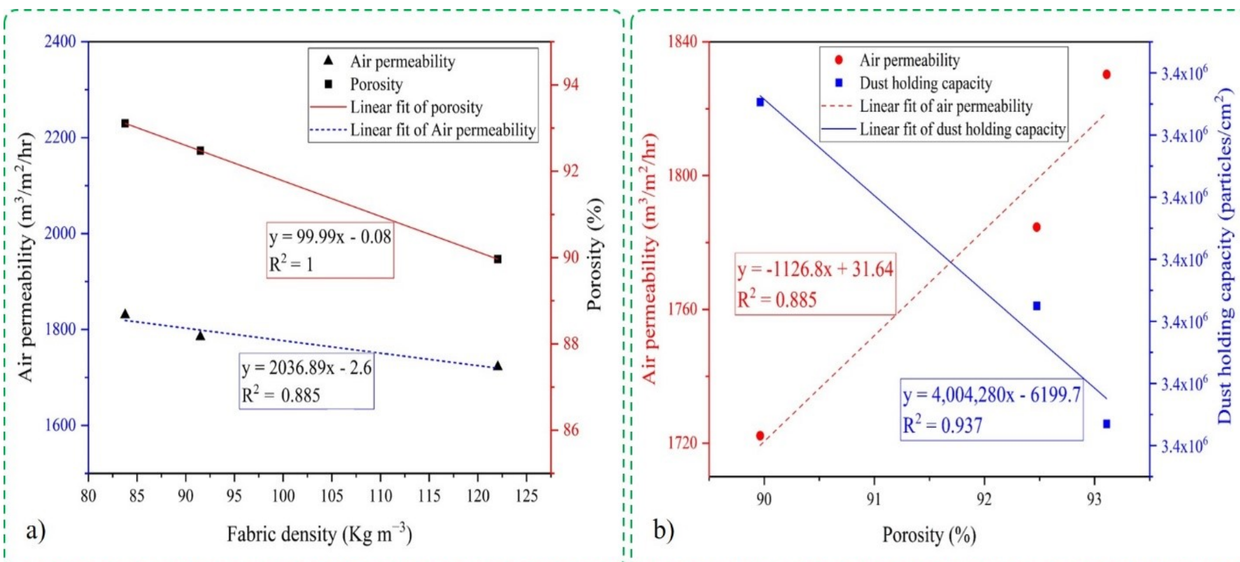

Figure 7. Relationship between properties of needle-punched nonwoven samples: a) linear fit of fabric density with air permeability and porosity, b) linear fit of porosity with air permeability and dust holding capacity

Table 4. Linear fit of properties of needle-punched nonwoven samples

x	y	Adjusted R^2	y = bx + a	Equation
Fabric density	Air permeability	0.885	y = 2086.39x - 2.6	(5)
Fabric density	Porosity	1	y = 99.99x - 0.08	(6)
Porosity	Air permeability	0.885	y = -1126.8x + 31.64	(7)
Porosity	Dust holding capacity	0.937	y = 4,004,280x – 6199.7	(8)

Relationship between Porosity, Air Permeability and Dust Holding Capacity

The linear fit relationship between porosity and air permeability and between porosity and the dust-holding capacity of needle-punched nonwoven samples is shown in Figure 7 (b) and Table 4. The linear fit analysis between the porosity (x) and air permeability (y) is indicated by equation (7). This equation proposes that as the porosity increases, the air permeability also increases, with a coefficient of 31.64. The coefficient of determination (R^2) for this linear fit was 0.885, indicating that approximately 88.5% of the variability in air permeability can be explained by the variation in porosity. The linear fit analysis between porosity (x) and dust-holding capacity (y) is presented in equation (8). This equation suggests that as porosity increases, the dust holding capacity decreases, with a coefficient of -6199.7. The coefficient of determination (R^2) for this linear fit was 0.937, indicating that approximately 93.7% of the variability in the dust-holding capacity can be explained by altering the porosity.

Effects of Fibre Composition and Properties on Hydrophobicity, Thermal Resistance and Dust-holding Capacity

The hydrophobic properties of needle-punched nonwoven samples are shown in Figure 8. Sample N6 (Figure 8 (d and i)), which had the highest water WCA of 133.12°, was composed of 60% PP fibres. PP fibres are recognized for their inherent hydrophobic nature, which can be attributed to the nonpolar structure of PP and the presence of methyl groups. Therefore, the high percentage of PP fibres in N6, combined with its hydrophobic properties, significantly contributes to its outstanding water repellency [37]. Sample N7 (Figure 8 e and j) closely followed a WCA of 132.40° and consisted of 60% PPS fibres. The hydrophobic nature of PPS can be attributed to its aromatic ring structure present in its molecular composition. This structure created a robust barrier against water, further enhancing the hydrophobic behaviour of the fibres. Consequently, the significant proportion of PPS fibres in N7, combined with their inherent hydrophobicity, resulted in good water repellency [41-43].

Sample N4 (Figure 8 (b and g)) exhibited a WCA of 125.04° and was composed of 60% PET fibres. PET fibres possess moderate hydrophobic properties, which explain the relatively high WCA observed in this sample. The hydrophobicity of PET can be attributed to its nonpolar molecular structure, which hinders water absorption. Hence, the substantial presence of PET fibres in N4, combined with their inherent hydrophobicity, significantly contributes to the water repellency of the sample [2,27,28]. Sample N3 (Figure 8 (a and f)) demonstrated a WCA of 120.90° and was comprised of 60% PAN fibres. PAN is considered moderately hydrophobic, primarily due to the presence of cyanoethyl groups in its molecular structure, which generates a slight repulsion towards water [18-21].

Sample N5 (Figure 8 (c & h)) displays the lowest WCA of 117.42° and consists of 60% PLA fibres. PLA fibres are well known for their biodegradability and typically demonstrate lower hydrophobicity compared to other synthetic fibres. This characteristic contributed to the lowest water contact angle observed for this sample. PLA's hydrophilic nature of PLA stems from the presence of polar functional groups, including hydroxyl (–OH) groups, within its molecular structure. These polar groups have an affinity for water molecules, making PLA fibres more prone to moisture absorption and less hydrophobic than the other fibres. While PLA can exhibit slight hydrophilic or hydrophobic behaviour, pure PLA is generally considered less hydrophobic, resulting in a lower water contact angle [36].

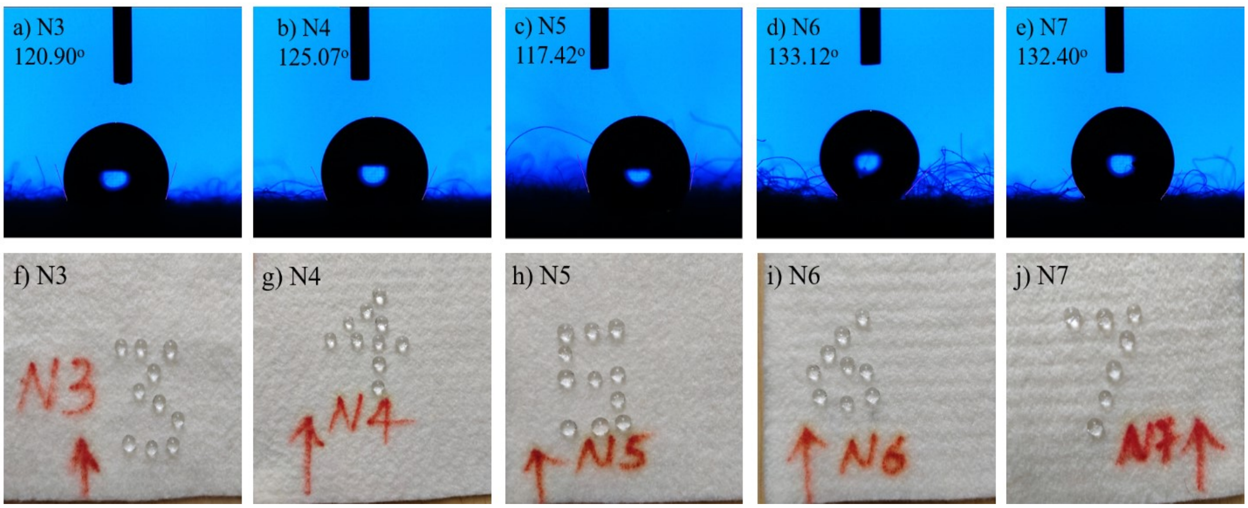

Figure 8. Hydrophobic properties of samples with different fibre composition: WCA of needle-punched nonwoven samples (a-e), water droplets on the surfaces of samples (f-j)

The thermal resistance properties of needle-punched nonwoven samples are shown in Table 5, namely N3, N4, N5, N6, and N7, which are influenced by various factors such as fibre fineness, inherent thermal resistance properties, composition, and fabric density. N7 is characterized by the highest thermal resistance (0.24255 $Wm^{-1}K^{-1}$) among the samples owing to its fabric density and 60% PPS fibre proportion. N3 also exhibited a higher thermal resistance (0.23236 $Wm^{-1}K^{-1}$) because of its denser structure and 60% PAN fibre composition. In contrast, N4 demonstrated thermal resistance (0.19569 $Wm^{-1}K^{-1}$) despite its relatively high fabric density. This sample comprised 60% PET fibres, offering a slightly lower inherent resistance compared to PAN and PPS. N5 with thermal resistance (0.18418 $Wm^{-1}K^{-1}$), consists mainly of 60% coarser PLA fibres, which likely impacts its thermal performance. With a fabric density of 81.70 Kg/m^3, N5 exhibited lower air entrapment, further reducing its thermal resistance. N6, which had the lowest thermal resistance (0.17490 $Wm^{-1}K^{-1}$), contained 60% PP fibres known for their moderate thermal resistance. Additionally, its fabric density of 86.42 Kg/m^3 is relatively low, potentially low air entrapment and contributing to its lower thermal resistance.

PAN, PPS, and PET fibres inherently offer good thermal resistance [22-25,29,41-43], whereas PP and PLA exhibit moderate resistance. Finer fibres, characterized by lower dtex values, generally create a more tortuous path for heat transfer, potentially enhancing thermal resistance. In addition, a higher fabric density signifies a greater amount of trapped air within the nonwoven structure, leading to improved thermal insulation. Samples with higher fabric density and a higher percentage of fibres with inherently higher thermal resistance tended to exhibit superior thermal insulation, while those with lower fabric density and a higher proportion of fibres with lower resistance demonstrated lower thermal resistance values.

Table 5. Tested properties of needle-punched nonwoven samples with different blend composition ratios

Samples	N3	N4	N5	N6	N7
Thickness (mm)	3.50	3.68	4.75	4.46	3.61
GSM	393.04	391.13	388.30	385.30	394.64
Fabric density (Kg/m^3)	112.44	106.27	81.70	86.42	109.36
Porosity (%)	90.75	91.26	93.28	92.89	91.01
Air permeability ($m^3/m^2/hr$)	1,749.22	1,773.38	1,916.46	1,829.87	1,761.97
Pressure drop (Pa)	74.05	70.85	61.25	64.48	72.89
Dust holding capacity ($particles/cm^2$)	3,439,773	3,434,771	3,423,000	3,427,579	3,437,779
Thermal resistance ($Wm^{-1}K^{-1}$)	0.23236	0.19569	0.18418	0.17490	0.24255

The dust-holding and pressure drop of the needle-punched nonwoven samples with different proportions are presented in Table 5. Among the samples, N3 stood out because of its high fabric density and a significant portion of PAN fibres (60%). PAN fibres with finer linear densities contributed to the compact structure of this sample. The combination of other fibres in N3 created diverse surface properties, which enhanced the retention of dust particles. The relatively high dust-holding capacity of 3,439,773 $particles/cm^2$ at a pressure drop of 74.05 pa suggests that the blend of fibre types and the higher fabric density were effective in capturing and retaining dust. N4, despite having a slightly lower fabric density than N3, maintained a relatively high dust-holding capacity of 3,434,771 $particles/cm^2$ at a pressure drop of 70.85 pa. This sample was dominated by PET fibres (60%), with relatively higher fineness and shorter length, contributing to the ability of the sample to retain dust particles within the fabric structure. N5, on the other hand, had the lowest fabric density among the samples because of the high percentage of PLA fibres (60%), which were relatively coarser and longer. However, it exhibited a comparable dust-holding capacity of 3,423,000 particles/cm² at a relatively low-pressure drop of 61.25 pa. The blending of other fibres with PLA and the rough surface of the PLA fibres (Figure 2 (c)) effectively trapped dust particles, and the lower fabric density allowed for a lower pressure drop.

N6 had a fabric density that was slightly higher than that of N5 and a higher percentage of PP fibres (60%). PP fibres are lightweight and hydrophobic, which contributes to their high thickness. This could explain the dust-holding capacity of 3,427,579 particles/cm² at a moderate pressure drop of 64.48 pa compared to others. Lastly, N7 had a higher fabric density composed of a higher percentage of PPS fibres (60%). PPS fibres are known for their high thermal stability and chemical resistance, which could contribute to the fabric's ability to retain dust particles. The dust-holding capacity of N7 was 3,437,779 particles/cm² at a pressure drop of 72.89 pa. Fibre properties like surface roughness and electrostatic charge, which can significantly impact dust adhesion will be the future work. For example, fibres with a rougher surface or inherent static charge might hold dust more effectively. Nevertheless, the study demonstrated the influence of fabric density, fibre types, and their proportions in the blend on the dust-holding capacity of the needle-punched nonwoven samples. The test results and studies [20,30,31,33,34,41] showed that the specific properties of each fibre type also played a significant role in determining the effectiveness of dust retention.

Statistical Analysis

The performance analysis of three needle-punched samples (N0, N1, and N2) was conducted to evaluate their characteristics, considering both web arrangement and fibre properties. Table 6 displayed the results in porosity, air permeability, dust-holding capacity, water contact angle and thermal resistance. N0, characterized by a cross-laid web arrangement, demonstrated statistically significant differences (p-value ≤ 0.05) in various parameters compared to N1 and N2. The cross-laid web structure likely influenced porosity, air permeability, dust-holding capacity, and thermal resistance. N1, with a parallel-laid arrangement, exhibited distinct performance characteristics, indicating the impact of the arrangement on the filtration media. N2, being pre-needled and parallel-laid, showed its unique set of properties, contributing to the overall comparison.

Table 6. Statistical analysis of needle-punched nonwoven samples

S/N	Tested Properties	N0	N1	N2	P-value	Tukey Test Sig N0-N1	Tukey Test Sig N0-N2	Tukey Test Sig N1-N2
1	Porosity (%)	89.96	92.47	93.11	0.024	0	1	0
2	Air permeability ($m^3/m^2/hr$)	1722.25	1784.61	1830.26	0.015	0	1	0
3	Dust holding capacity (particles/cm^2)	3,446,119	3,432,995	3,425,400	0.000	1	1	0
4	Water contact angle (°)	126.77	126.47	126.56	0.664	0	0	0
5	Thermal resistance (m^2KW^{-1})	0.21053	0.20820	0.19914	0.027	0	1	0

- P-value ≤ 0.05 indicates that at 0.05 level, the population means are significantly different.
- Sig equals 1 indicates that the difference of the means is significant at 0.05 level.
- Sig equals 0 indicates that the difference of the means is not significant at 0.05 level.

The selection of fibres, including polyphenylene sulfide (PPS), polypropylene (PP), polyester (PET), polylactic acid (PLA), and polyacrylonitrile (PAN), being blended in equal proportions, played a vital role in determining the final performance of each sample. These fibre properties likely provided the observed variations in porosity, air permeability, dust-holding capacity, and thermal resistance among the samples. Notably, the water contact angle exhibited no statistically significant differences, indicating that the water repellency of the samples remained consistent across the different web arrangements. The water contact angle had no statistically significant results ($p = 0.664$) at the level of 0.05. The lack of significant difference in water contact angle suggested that it was primarily influenced by the fibre blend's chemistry rather than the web arrangement. Overall, the study provided valuable insights into how the combination of web arrangement and specific fibre properties influenced the performance of needle-punched samples in various key parameters for filtration applications.

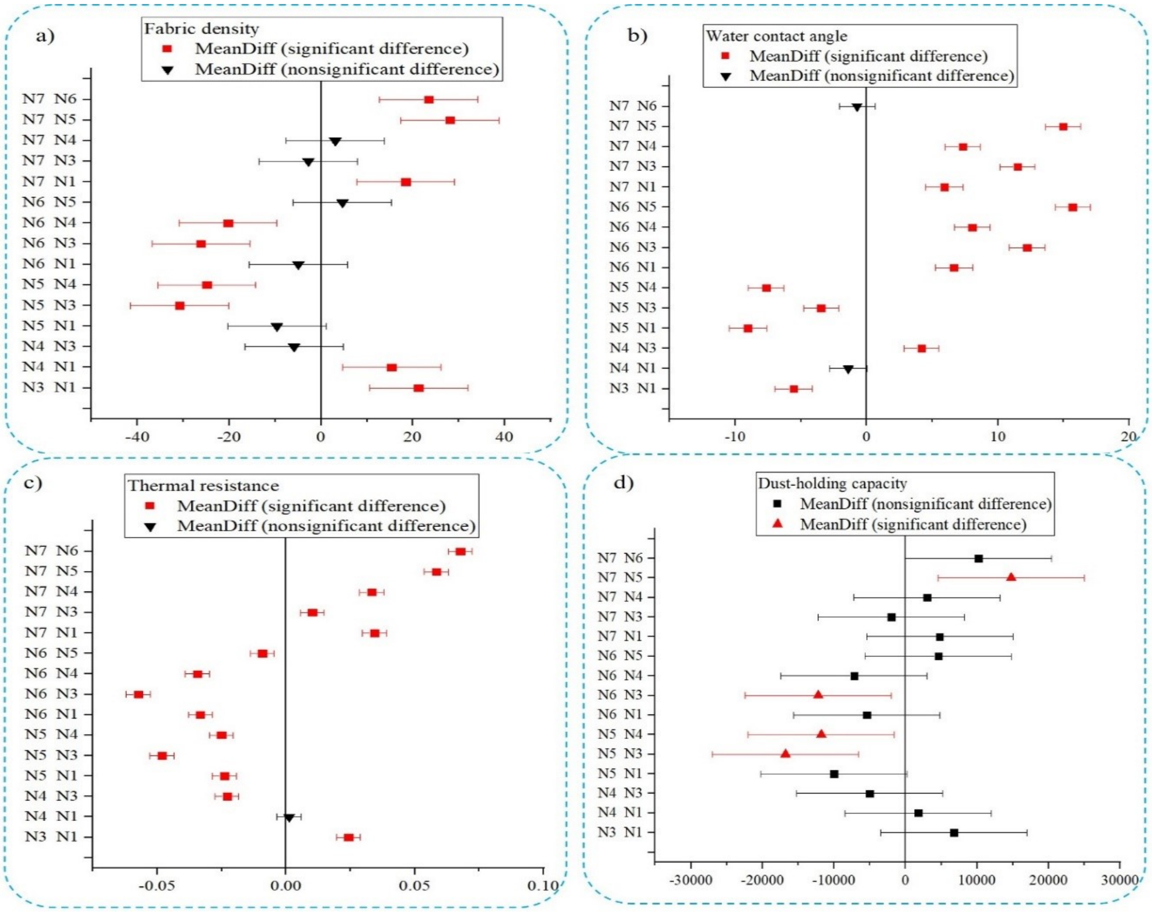

Figure 9. Mean comparison plot Turkey analysis: a) fabric density, b) water contact angle, c) thermal resistance, d) dust-holding capacity

The Tukey analysis conducted on the data in Figure 9 revealed several significant findings regarding the properties of the needle-punched nonwoven samples, which have the same web arrangement with different fibre blend compositions. Firstly, for hydrophobicity and thermal resistance, the mean difference between almost all interactions with the samples was significantly different. This indicated that variations in these properties were likely influenced by inherent fibre properties and the blending ratio of the fibres within the samples. The significant differences observed suggest that specific combinations of fibre types and proportions have a substantial impact on the hydrophobicity and thermal resistance of nonwoven materials. Secondly, concerning fabric density, the analysis indicated that the mean difference between the majority of interactions within samples, which exhibited significant differences in fibre fineness, was also significant. This suggests that fabric density is closely related to fibre fineness, with variations in the thickness of individual fibres affecting the overall density of the fabric. The significant differences observed in fabric density among samples with different fibre fineness highlight the importance of considering both factors in determining the structural characteristics of the nonwoven materials. Lastly, the Tukey analysis revealed significant mean differences in dust-holding capacity between four interactions within samples that exhibited significant differences in fabric density. This suggested that dust-holding capacity was influenced by both fibre fineness and fabric density. The variations in dust-holding capacity among samples with different fabric densities indicated that the arrangement and density of fibres within the nonwoven structure played a crucial role in determining its ability to retain dust particles. Overall, the analysis helped to elucidate the factors contributing to the overall performance and functionality of the nonwoven materials, thus informing future research and development efforts in this area.

CONCLUSION

In this article, the air filtration, hydrophobic and thermal properties of needle-punched nonwovens produced by blending PAN, PET, PLA, PP, and PPS with different web arrangements were investigated. This was a novel approach for $PM_{2.5}$ filtration on five fibres blended needle-punched structures. The cross-laid web arrangement of sample N0 resulted in the lowest porosity (89.96%), air permeability (1722.25 $m^3/m^2/hr$) and high dust holding capacity of 3,372,082 particles/cm^2 due to its high fabric density and compact structure. Sample N2, which underwent pre-needling and parallel-laid arrangement, displayed the highest porosity (93.11%) and air permeability (1830.26 $m^3/m^2/hr$) due to its lower fabric density. Sample N3, 60% PAN fibres with finer linear density led to a high dust holding capacity of 3,368,490 particles/cm^2. In contrast, N5, 60% PLA fibres with coarser linear density and lowest fabric density, exhibited a comparable dust holding capacity of 3,336,951 particles/cm^2.

Water contact angles observed among N0, N1 and N3 were consistent at around 126.5° for all samples, suggesting similar water-repellency properties. On the other hand, Sample N6, composed of 60% Polypropylene (PP) fibres, had the highest WCA of 133.12°. This is because inherent hydrophobic nature of PP due to its non-polar structure and methyl groups. In contrast, Sample N5 with 60% Polylactic acid (PLA) fibres, had the lowest WCA of 117.42°, due to PLA's hydrophilic nature from its polar functional groups. The results showed that inherent fibre hydrophobicity and proportion of bled of fibres have effects on the hydrophobicity of samples than web arrangement and density of fabric. When fibres blended in equal proportion, Sample N0, characterized by a cross-web arrangement and the highest fabric density, exhibited the highest thermal resistance (0.21053 $m^2 \cdot K/W$). N7 is characterized by the highest thermal resistance among the samples (0.24255 $Wm^{-1}K^{-1}$) and is composed of 60% PPS fibres. N6 (with the lowest thermal resistance of 0.17490 $Wm^{-1}K^{-1}$) contains 60% PP fibres. Samples with higher fabric density and a higher percentage of fibres with inherently higher thermal resistance, such as PAN and PPS, tended to exhibit superior thermal insulation, while those with lower fabric density and a higher proportion of fibres with lower resistance, such as PP and PLA, demonstrated lower thermal resistance values.

As fabric density increased, air permeability decreased with a coefficient of -2.6, and porosity decreased with a coefficient of -0.8. These relationships had high coefficients of determination (adjusted R^2 of 0.885 and 1.0, respectively), indicating that the changes in fabric density could explain a large proportion of the variability in air permeability and porosity. The sample with a cross-laid web arrangement (N0) demonstrated statistically significant differences in various parameters, including porosity, air permeability, dust holding capacity, and thermal resistance, compared to the samples with parallel-laid arrangements (N1 and N2). This suggested that the web arrangement played a crucial role in the filtration media's performance. The selection of fibres, including PPS, PP, PET, PLA, and PAN, blended in equal proportions, also contributed to the observed variations in the samples' properties. These fibre properties likely influenced the porosity, air permeability, dust holding capacity, thermal resistance and mechanical properties. The water contact angle did not show any statistically significant differences among the samples which were blended in equal fibres proportion, indicating that the water repellency was primarily influenced by the fibre blend's chemistry rather than the web arrangement. The hydrophobicity of samples N5 and N6 strengthen this conclusion. Hence, hydrophobicity and thermal resistance properties played a vital role for $PM_{2.5}$ filters in automobile cabins, engines, and indoor applications, as they could prevent moisture ingress and microbial growth, and ensure stability against temperature fluctuations.

Author Contributions

Conceptualization – Yesuf HM, Xiaohong Q, Xueping Z; methodology – Yesuf HM; formal analysis – Yesuf HM; investigation – Yesuf HM; writing-original draft preparation – Yesuf HM; writing-review and editing – Yesuf HM, Islam SR, Semanie DM, Jhatial AK, Xiaohong Q, Xueping Z; validation and project administration – Xiaohong Q, Xueping Z. All authors have read and agreed to the published version of the manuscript.

Conflicts of Interest

The authors declare no conflict of interest.

Funding

This work was partly supported by a grant (51973027) from the National Natural Science Foundation of China, and the International Cooperation Fund of Science and Technology Commission of Shanghai Municipality (21130750100). This work has also been supported by the Chang Jiang Scholars Program and the Innovation Program of Shanghai Municipal Education Commission (2019-01-07-00-03-E00023) to Prof. Xiaohong Qin, and the DHU Distinguished Young Professor Program to Prof. Xueping Zhang.

Acknowledgements

The authors would like to acknowledge the National Natural Science Foundation of China, International Cooperation Fund of Science and Technology Commission of Shanghai Municipality, Innovation Program of Shanghai Municipal Education Commission, Donghua University and Bahir Dar University, EiTEX.

REFERENCES

[1] Yesuf HM, Memon H, Islam SR, Jiawei L, Atalie D, Zhang X, Qin X. Blend of Fibres to Improve the Mechanical Properties of Needle-Punched Nonwovens for PM2.5 Air Filtration. Textile & Leather Review. 2024; 7:235-264. https://doi.org/10.31881/TLR.2024.004

[2] Boominathan S, Bhuvaneshwari M, Sangeetha K, Pachiyappan K, Devaki E. Influence of fibre blending on thermal and acoustic properties nonwoven material. Journal of Natural Fibres. 2022; 19(15):11193-11203. https://doi.org/10.1080/15440478.2021.2021123

[3] Hemamalini T, Giri Dev V. Wet laying nonwoven using natural cellulosic fibres and their blends: process and technical applications. A review. Journal of Natural Fibres. 2021; 18(11):1823-1833. https://doi.org/10.1080/15440478.2019.1701606

[4] Egan J, Salmon S. Strategies and progress in synthetic textile fibre biodegradability. SN Applied Sciences. 2022; 4:1-36. https://doi.org/10.1007/s42452-021-04851-7

[5] Ahmad Z, Naeem MS, Jabbar A, Irfan M. Fibres for Other Technical Textiles Applications. In: Ahmad S, Rasheed A, Nawab Y, editors. Fibres for Technical Textiles. Cham: Springer International Publishing; 2020. p. 201-220. https://doi.org/10.1007/978-3-030-49224-3_10

[6] Li X, Yang Q, Zhang K, Pan L, Feng Y, Jia Y, Xu N. Property improvement and compatibilization mechanism of biodegradable polylactic acid/maleic anhydride-based/polypropylene spunbonded nonwoven slices. Journal of Cleaner Production. 2022; 375:134097. https://doi.org/10.1016/j.jclepro.2022.134097

[7] Rasheed A, Zehra H, Ahmad S, Ahmad F. Development of multi-layer needle-punched nonwoven

electric heating pad. The Journal of The Textile Institute. 2022; 114(3):462-469. https://doi.org/10.1080/00405000.2022.2049049

[8] Thenmozhi R, Thilagavathi G. Investigations on Kapok/Polypropylene Needle Punched Nonwoven for Thermal Resistance Applications. Journal of Natural Fibres. 2023; 20(1):2146247. https://doi.org/10.1080/15440478.2022.2146247

[9] Wang W, Feng L, Song B, Wang L, Shao R, Xia Y, Liu D, Li T, Liu S, Xu Z. Fabrication and application of superhydrophobic nonwovens: a review. Materials Today Chemistry. 2022; 26:101227. https://doi.org/10.3390/polym12122836

[10] Wei DW, Wei H, Gauthier AC, Song J, Jin Y, Xiao H. Superhydrophobic modification of cellulose and cotton textiles: Methodologies and applications. Journal of Bioresources and Bioproducts. 2020; 5(1):1-15. https://doi.org/10.3390/polym12122836

[11] Liang L, Wen T, Xin J, Su C, Song K, Zhao W, Liu H, Su G. Fluoropolymer: A Review on Its Emulsion Preparation and Wettability to Solid-Liquid Interface. Molecules. 2023; 28(2):905. https://doi.org/10.3390/molecules28020905

[12] Belov NA, Alentiev AY, Bogdanova YG, Vdovichenko AY, Pashkevich DS Direct Fluorination as Method of Improvement of Operational Properties of Polymeric Materials. Polymers, 2020. 12. https://doi.gov/10.3390/polym12122836

[13] Ghasem N. Toxicity aspects, disposal, recycling, environmental, safety, and health issues of fluoropolymer nanocomposites. editors. Advanced Fluoropolymer Nanocomposites. Elsevier; 2023. p. 809-820. https://doi.org/10.1016/B978-0-323-95335-1.00014-1

[14] Korzeniowski SH, Buck RC, Newkold RM, kassmi AE, Laganis E, Matsuoka Y, Dinelli B, Beauchet S, Adamsky F, Weilandt K. A critical review of the application of polymer of low concern regulatory criteria to fluoropolymers II: fluoroplastics and fluoroelastomers. Integrated Environmental Assessment and Management. 2023; 19(2):326-354. https://doi.org/10.1002/ieam.4646

[15] Henry BJ, Carlin JP, Hammerschmidt JA, Buck RC, Buxton LW, Fiedler H, Seed J, Hernandez O. A critical review of the application of polymer of low concern and regulatory criteria to fluoropolymers. Integrated Environmental Assessment and Management. 2018; 14(3):316-334. https://doi.org/10.1002/ieam.4035

[16] Brennan NM, Evans AT, Fritz MK, Peak SA, von Holst HE. Trends in the regulation of per-and polyfluoroalkyl substances (PFAS): a scoping review. International journal of environmental research and public health. 2021; 18(20):10900. https://doi.org/10.3390/ijerph182010900

[17] Chohan A, Petaway H, Rivera-Diaz V, Day A, Colaianni O, Keramati M. Per and polyfluoroalkyl substances scientific literature review: water exposure, impact on human health, and implications for regulatory reform. Reviews on Environmental Health. 2021; 36(2):235-259. https://doi.org/10.1515/reveh-2020-0049

[18] Tian Z, Lei Y, Fan Y, Zhou P, Liu F, Zhu Z, Sun H, Liang W, Li A. Efficient capture of PM 2.5 by intertwined tubular conjugated microporous polymer-based filters with high stability in a humid environment. Journal of Materials Chemistry A. 2021; 9(12):7703-7711. https://doi.org/10.1039/d0ta11908c

[19] Yang X, Pu Y, Li S, Liu X, Wang Z, Yuan D, Ning X. Electrospun polymer composite membrane with superior thermal stability and excellent chemical resistance for high-efficiency PM2. 5 capture. ACS applied materials & interfaces. 2019; 11(46):43188-43199. https://doi.org/10.1021/acsami.9b15219

[20] Jing L, Shim K, Toe CY, Fang T, Zhao C, Amal R, Sun K-N, Kim JH, Ng YH. Electrospun polyacrylonitrile–ionic liquid nanofibres for superior PM2. 5 capture capacity. ACS applied materials & interfaces. 2016; 8(11):7030-7036. https://doi.org/10.1021/acsami.5b12313

[21] Zhang P, Wan D, Zhang Z, Wang G, Hu J, Shao G. RGO-functionalized polymer nanofibrous membrane with exceptional surface activity and ultra-low airflow resistance for PM 2.5 filtration. Environmental Science: Nano. 2018; 5(8):1813-1820. https://doi.org/10.1039/C8EN00468D

[22] Bourbigot S, Flambard X. Heat resistance and flammability of high performance fibres: A review. Fire and Materials. 2002; 26(4-5):155-168. https://doi.org/10.1002/fam.799

[23] Kumar N, Kaliappan S, Socrates S, Natrayan L, Patel PB, Patil PP, Sekar S, Mammo WD. Investigation of Mechanical and Thermal Properties on Novel Wheat Straw and PAN Fibre Hybrid Green Composites. International Journal of Chemical Engineering. 2022; 2022:3598397. https://doi.org/10.1155/2022/3598397

[24] Sas I, Gorga RE, Joines JA, Thoney KA. Literature review on superhydrophobic self-cleaning surfaces produced by electrospinning. Journal of Polymer Science Part B: Polymer Physics. 2012; 50(12):824-845. https://doi.org/10.1002/polb.23070

[25] Shi S, Si Y, Han Y, Wu T, Iqbal MI, Fei B, Li RKY, Hu J, Qu J. Recent Progress in Protective Membranes Fabricated via Electrospinning: Advanced Materials, Biomimetic Structures, and Functional Applications. Advanced Materials. 2022; 34(17):2107938. https://doi.org/10.1002/adma.202107938

[26] Vatanpour V, Pasaoglu ME, Kose-Mutlu B, Koyuncu I. Polyacrylonitrile in the Preparation of Separation Membranes: A Review. Industrial & Engineering Chemistry Research. 2023; 62(17):6537-6558. https://doi.org/10.1021/acs.iecr.3c00057

[27] Orasugh JT, Bal K, Chattopadhyay D, Ghosh SK, Ray SS. Optimization of Fabric Parameters on the Effectual Properties of Nonwoven Industrial Wipes Blend using Response Surface Methodology. Indian Journal of Fibre and Textile Engineering (IJFTE). 2022; 2(2):1-9. https://doi.org/10.54105/ijfte.C2401.111422

[28] Huijing Z, Zhang Y. Water-repellent and lipophilic composite needle-punched nonwoven fabric and preparation method thereof. US20210404114A1 [Patent] 2022.

[29] Mohd Tahir AA-h, Abdul Rashid AH, Nasir SH, Ahmad M, Nor Anuwar AA. Thermal resistance and bursting strength analysis of multilayer needle-punched bamboo/polyester nonwoven batt. The Journal of The Textile Institute. 2023; 114(7):974-985. https://doi.org/10.1080/00405000.2022.2105069

[30] Kurtz O, Meyer J, Kasper G. The contribution of small leaks in a baghouse filter to dust emission in the PM2.5 range—A system approach. Particuology. 2017; 30:40-52. https://doi.org/10.1016/j.partic.2016.08.001

[31] Singh P, Mukhopadhyay A, Gupta P. Performance of surface finished polyester filter media exposed to different dust types with the variation of dust concentration. Powder Technology. 2023; 426:118614. https://doi.org/10.1016/j.powtec.2023.118614

[32] Mewoli A, Segovia C, Soppie AG, Ebanda FB, Njom AE, Ateba A, Brosse N. Investigation of the performance of needle-punched nonwoven fabrics using Triumfetta cordifolia and thermoplastic fibres, compared to other commercial bast fibres used in preformed biosourced composites. Heliyon. 2023; 9(7): e17888. https://doi.org/10.1016/j.heliyon.2023.e17888

[33] Farrington D, Lunt J, Davies S, Blackburn R. Poly (lactic acid) fibres. In: Blackburn R, editors. Biodegradable and sustainable fibres. USA: Taylor & Francis; 2005. p. 191-218. Available from: https://books.google.com/books?hl=en&lr=&id=Sk-kAgAAQBAJ&oi=fnd&pg=PA191&dq=Poly(lactic+acid)+fibres+&ots=KLBwTC3n8i&sig=IGKitfgitYSnS39PbsLjZQquDBE#v=onepage&q=Poly(lactic%20acid)%20fibres&f=false

[34] Yang Y, Zhang M, Ju Z, Tam PY, Hua T, Younas MW, Kamrul H, Hu H. Poly (lactic acid) fibres, yarns and fabrics: Manufacturing, properties and applications. Textile Research Journal. 2021; 91(13-14):1641-1669. https://doi.org/10.1177/0040517520984101

[35] Fang C-c, Zhang Y, Qi S-y, Li Y-y, Wang P. Characterization and analyses of degradable composites made with needle-punched jute nonwoven and polylactic acid (PLA) membrane. Cellulose. 2020; 27(10):5971-5980. https://doi.org/10.1007/s10570-020-03204-8

[36] Rajakaruna RADNV, Subeshan B, Asmatulu E. Fabrication of hydrophobic PLA filaments for additive manufacturing. Journal of Materials Science. 2022; 57(19):8987-9001. https://doi.org/10.1007/s10853-022-07217-5

[37] Brindha R, Thilagavathi G, Viju S. Development of nettle–polypropylene-blended needle-punched nonwoven fabrics for oil spill cleanup applications. Journal of Natural Fibres. 2019:1439-1453. https://doi.org/10.1080/15440478.2019.1578717

[38] Muthukumar N, Thilagavathi G, Kiruba T. Effect of bonding techniques on thermal insulation and biodegradation of banana fibre/recycled polyester nonwovens. Journal of Reinforced Plastics and Composites. 2023:073168442311621-073168442311621. https://doi.org/10.1177/07316844231162138

[39] Li T-T, Fan Y, Cen X, Wang Y, Shiu B-C, Ren H-T, Peng H-K, Jiang Q, Lou C-W, Lin J-H. Polypropylene/Polyvinyl Alcohol/Metal-Organic Framework-Based Melt-Blown Electrospun Composite Membranes for Highly Efficient Filtration of PM2.5. Nanomaterials. 2020; 10(10):2025. https://doi.org/10.3390/nano10102025

[40] Rajak A, Syahputra TS, Munir MM, Khairurrijal K. The Effect of Nonwoven Microfibre Substrate Polypropylene Thickness to Air Filtration Performance of Polyacrilonitrille Nanofibre. Jurnal ILMU DASAR. 2019(2):95-104%V 20. https://doi.org/10.19184/jid.v20i2.9658

[41] Zhao P, Yan J, Chen C, Zhang H, Wu M, Yao S, Jia Y, Wang H, Xiong S, Wang L. PPS ultrafine fibre enhanced aramid fibre filter with superior thermal stability and excellent chemical resistance for efficient PM2.5 removal. Reactive and Functional Polymers. 2023; 188:105605. https://doi.org/10.1016/j.reactfunctpolym.2023.105605

[42] Wang Y, Xu Y, Wang D, Zhang Y, Zhang X, Liu J, Zhao Y, Huang C, Jin X. Polytetrafluoroethylene/Polyphenylene Sulfide Needle-Punched Triboelectric Air Filter for Efficient Particulate Matter Removal. ACS Applied Materials & Interfaces. 2019; 11(51):48437-48449. https://doi.org/10.1021/acsami.9b18341

[43] Bai M, Wang J, Zhou R, Lu Z, Wang L, Ning X. Polyphenylene sulfide fabric with enhanced oxidation resistance and hydrophobicity through polybenzoxazine surface coating for emission control in harsh environment. Journal of Hazardous Materials. 2022; 432:128735. https://doi.org/10.1016/j.jhazmat.2022.128735

[44] Mudoi MP, Singh V, Kaur H, Choudhary A. Chapter 10 Advanced fibre materials in textile. In: Jeenat A, Chandrabhan V, editors. Fibre Materials. Berlin, Boston: De Gruyter; 2023. p. 259-272. https://doi.org/10.1515/9783110992892-010

[45] Maity S, Singha K, Pandit P. 1 - Introduction to functional and technical textiles. In: Maity S, Singha K, Pandit P, editors. Functional and Technical Textiles. Woodhead Publishing; 2023. p. 1-30. https://doi.org/10.1016/B978-0-323-91593-9.00021-3

[46] Shim E, Noh J, Kim Y. Development and Performance Evaluation of Polytetrafluoroethylene-Membrane-Based Automotive Cabin Air Filter. ACS Omega. 2022; 7(48):43738-43746. https://doi.org/10.1021/acsomega.2c04758

[47] Xu B, Wu Y, Lin Z, Chen Z. Investigation of Air Humidity Affecting Filtration Efficiency and Pressure Drop of Vehicle Cabin Air Filters. Aerosol and Air Quality Research. 2014; 14(3):1066-1073. https://doi.org/10.4209/aaqr.2013.06.0204

[48] Wei S, He Y, Yin W, Tian C, Jiao P, Bian J. Study on Performance of Cabin Air filters Under Different Work Conditions. Journal of Physics: Conference Series. 2021; 1885(2):022054. http://doi.org/10.1088/1742-6596/1885/2/022054

[49] He X, Brem BT, Bahk YK, Kuo Y-Y, Wang J. Effects of relative humidity and particle type on the performance and service life of automobile cabin air filters. Aerosol Science and Technology. 2016; 50(6):542-554. https://doi.org/10.1080/02786826.2016.1167832

[50] Dziubak T, Dziubak SD. Experimental Study of Filtration Materials Used in the Car Air Intake. Materials. 2020; 13(16):3498. https://doi.org/10.3390/ma13163498

[51] Dziubak T, Dziubak SD. A Study on the Effect of Inlet Air Pollution on the Engine Component Wear and Operation. Energies. 2022; 15(3):1182. https://doi.org/10.3390/en15031182

[52] Dziubak T, Karczewski M. Experimental Study of the Effect of Air Filter Pressure Drop on Internal Combustion Engine Performance. Energies. 2022; 15(9):3285. https://doi.org/10.3390/en15093285

[53] Xu H, Jin W, Luo J, Wang F, Zhu H, Liu G, Yu Y, Lei C, Guo Y. Study of the PTFE multi-tube high efficiency air filter for indoor air purification. Process Safety and Environmental Protection. 2021; 151:28-38. https://doi.org/10.1016/j.psep.2021.05.007

[54] Tang P, Ma P, Weng S, Zhou Y. Application of filter media surface hydrophobic modification to reduce bioclogging in the infiltration system. Environmental Technology. 2023; 44(15):2270-2279. https://doi.org/10.1080/09593330.2022.2026487

[55] Liu T, Cai C, Ma R, Deng Y, Tu L, Fan Y, Lu D. Super-hydrophobic Cellulose Nanofibre Air Filter with Highly Efficient Filtration and Humidity Resistance. ACS Applied Materials & Interfaces. 2021; 13(20):24032-24041. https://doi.org/10.1021/acsami.1c04258

[56] Roig O, Cuerva E, Pardal C, Guardo A, Isalgue A, Lopez-Besora J. Thermal Assessment of a Ventilated Double Skin Façade Component with a Set of Air Filtering Photocatalytic Slats in the Cavity. Buildings. 2023; 13(2):272. https://doi.org/10.3390/buildings13020272

[57] Yilmaz ND, Banks-Lee P, Powell NB, Michielsen S. Effects of porosity, fibre size, and layering sequence on sound absorption performance of needle-punched nonwovens. Journal of Applied Polymer Science. 2011; 121(5):3056-3069. https://doi.org/10.1002/app.33312

[58] American Society for Testing and Materials. ASTM C 830-00- Standard Test Methods for Apparent Porosity, Liquid Absorption, Apparent Specific Gravity, and Bulk Density of Refractory Shapes by Vacuum Pressure. 2000. https://doi.org/10.1520/C0830-00R16

[59] Gajjar C, King M, Guidoin R. Retrieval studies for medical biotextiles. editors. Biotextiles as Medical Implants. Elsevier; 2013. p. 182-210. https://doi.org/10.1533/9780857095602.1.182

[60] Maduna L. Development of spunlaced nonwoven filters from PAN, PPS and PI fibres for industrial use [dissertation]. South Africa: Nelson Mandela University; 2018. 179 p. Available from: https://core.ac.uk/download/pdf/224301116.pdf.

[61] Islam SR, Yu W, Naveed T. Influence of silica aerogels on fabric structural feature for thermal isolation properties of weft-knitted spacer fabrics. Journal of Engineered Fibres and Fabrics. 2019; 14:1558925019866446. https://doi.org/10.1177/1558925019866446

[62] Islam SR, Wang W, Junjie P, Jiang J, Shao H, Chen N. Study on thermal, mechanical, and wettability properties of three-dimensional weft-knitted spacer fabrics with various silica aerogels coating. Textile Research Journal. 2023; 93(15-16):3611-3629. https://doi.org/10.1177/00405175231161777